

Amazonian former gold mined soils as a source of methylmercury: Evidence from a small scale watershed in French Guiana

Stephane Guedron^{a, *}, Michel Grimaldi^b, Catherine Grimaldi^{c, d}, Daniel Cossa^e, Delphine Tisserand^a
and Laurent Charlet^a

^a IRD, Institut des Sciences de la Terre (ISTerre), UMR5559 (IRD/UJF/CNRS), University Joseph Fourier, BP 53, F-38041 Grenoble, France

^b IRD, UMR Bioemco-Biogéochimie et Ecologie des Milieux Continentaux, UMR211, Institut de Recherche pour le Développement, 32 avenue Henri Varagnat, F-93143 Bondy, France

^c INRA, UMR1069, Soil Agro and Hydrosystem, F-35000 Rennes, France

^d Agrocampus Rennes, UMR1069, Soil Agro and Hydrosystem, F-35000 Rennes, France

^e IFREMER, Laboratoire de Biogéochimie des Contaminants Métalliques, Centre de Méditerranée, BP 330, Zone Portuaire de Brégaillon, F-83507 La Seyne-sur-mer, France

*: Corresponding author : Stephane Guedron, Tel.: +33 0 4 76 63 59 28, fax: +33 0 4 76 63 52 52,
email address : stephane.guedron@ujf-grenoble.fr

Abstract:

Total mercury (HgT) and monomethylmercury (MMHg) were investigated in a tropical head watershed (1 km²) of French Guiana. The watershed includes a pristine area on the hill slopes and a former gold mined flat in the bottomland. Concentrations of dissolved and particulate HgT and MMHg were measured in rain, throughfall, soil water and at three points along the stream. Samples were taken in-between and during 14 storm events at the beginning and middle of the 2005 and 2006 rainy seasons. Dissolved and particulate HgT concentrations in the stream slightly increased downstream, while dissolved and particulate MMHg concentrations were low at the pristine sub-watershed outlet (median = 0.006 ng L⁻¹ and 1.84 ng g⁻¹, respectively) and sharply increased at the gold mined flat outlet (median = 0.056 ng L⁻¹ and 6.80 ng g⁻¹, respectively). Oxisols, which are dominant in the pristine area act as a sink of HgT and MMHg from rain and throughfall inputs. Hydromorphic soils in the flat are strongly contaminated with Hg (including Hg⁰ droplets) and their structure has been disturbed by former gold-mining processes, leading to multiple stagnant water areas where biogeochemical conditions are favorable for methylation. In the former gold mined flat high dissolved MMHg concentrations (up to 0.8 ng L⁻¹) were measured in puddles or suboxic soil pore waters, whereas high dissolved HgT concentrations were found in lower Eh conditions. Iron-reducing bacteria were suggested as the main methylators since highest concentrations for dissolved MMHg were associated with high dissolved ferrous iron concentrations. The connection between saturated areas and stagnant waters with the hydrographic network during rain events leads to the export of dissolved MMHg and HgT in stream waters, especially at the beginning of the rainy season. As both legal and illegal gold-mining continues to expand in French Guiana, an increase in dissolved and particulate MMHg emissions in the hydrographic network is expected. This will enhance MMHg bio-amplification and present a threat to local populations, whose diet relies mainly on fish.

Highlights :

- ▶ Mercury and monomethylmercury were investigated in a tropical head watershed of French Guiana.
- ▶ The pristine area covered by oxisol acted as a sink for both species from rain and throughfall inputs.
- ▶ Hg contaminated soils of the former gold-mining flat were identified as a source of methylmercury.
- ▶ Monomethylmercury was mainly produced at the beginning of the rainy season and released latter on.
- ▶ As gold-mining continues to expand, an enhancement of methylmercury bio-amplification is expected.

Keywords : Mercury; Methylmercury; Tropical watershed; Gold placers; Stream water; Oxisols; Hydromorphic soils

53 **1. Introduction**

54 Mercury (Hg) contamination of Amazonian ecosystems through the use of elemental Hg for
55 gold amalgamation has been highlighted by many scientific studies (Dorea et al., 2007,
56 Lechler et al., 2000, Malm, 1998, Pfeiffer et al., 1993, Roulet et al., 1999b, Wasserman et al.,
57 2003). Toxicological concerns related to high monomethyl-mercury (MMHg) concentrations
58 in Amazonian fish have been evidenced for Amerindian populations whose diet relies mainly
59 on fish (Brabo et al., 2000, Durrieu et al., 2005, Frery et al., 2001, Harper et al., 2008,
60 Porvari, 1995).

61 The main sources of MMHg have been identified in areas where oxygen content drops
62 sharply, such as river and lake sediments, as well as in lake water columns at the oxyclines
63 and in temperate flooded environments (Coquery et al., 2003, Hall et al., 2008). Amazonian
64 ecosystems combine most of the surrounding geochemical conditions favourable for Hg
65 methylation such as high temperature, high organic-matter content, abundant electron
66 acceptors (i.e., sulfate ions and ferric iron contents), and intensive microbial activities (Benoit
67 et al., 2003, Ullrich et al., 2001). Nevertheless, most studies performed in Amazonian
68 watersheds have focused on total Hg distribution in waters, river sediments and soils (Barbosa
69 et al., 2003, Dorea et al., 2007, Marchand et al., 2006, Roulet et al., 1998b) and few data are
70 available for MMHg. It is important to gain knowledge about Hg methylation in tropical
71 watersheds since correlations found between total Hg and MMHg concentrations are
72 commonly weak and related to external environmental factors, such as the chemical form of
73 Hg^{II} , which have a strong influence on its bioavailability for methylation (Birkett et al., 2005,
74 Lambertsson et al., 2006, Ullrich et al., 2001). The presence of elemental Hg is also an
75 important factor which must be considered in gold-mining areas, since Dominique et al.
76 (2007) have recently shown that, under experimental conditions, the presence of elemental Hg
77 droplets can enhance MMHg production.

78 In this study, we examined if MMHg was produced in flooded soils of a former gold mined
79 area and tested in the field the experimental findings of Dominique et al. (2007) regarding Hg
80 methylation in the presence of Hg⁰ droplets. We focussed on particulate and dissolved HgT
81 and MMHg outputs from a small watershed covered by tropical humid vegetation. This
82 watershed was chosen (i) because it includes a pristine area and a Hg contaminated former
83 goldmined flat, and (ii) because of its small scale (1 km²), which enables an optimal
84 understanding of Hg distribution in and between the different pedological and hydrological
85 compartments. Finally, we attempted to analyse the influence of internal (i.e., geochemical,
86 hydrological, geomorphological) and external (i.e., seasonality) determinants on Hg
87 methylation and emissions to the watershed's hydrological network.

88

89 **2. Site, material and methods**

90 **2.1 Environmental settings**

91 **Location:** The study site is the *Combat* Creek (CC) watershed, located in French Guiana,
92 South America (52°23'W, 4°35'N) (Fig. 1), covered by tropical rain forest. Its surface area is
93 approximately 1 km². The climate is tropical-humid with a mean annual rainfall of 4000 mm
94 (Barret, 2004). Precipitation mainly occurs from December to July, with May and June as the
95 wettest months.

96 **Bedrock:** The CC watershed is located in the 'Amina series' of the Guiana Proterozoic shield
97 consisting primarily of dark schist and thin sandstone (Milési et al., 1995). Vast gravel
98 deposits from ancestral rivers within the valleys contain large quantities of placer gold,
99 derived from the weathering of gold-quartz veins.

100 **Soil cover:** Soil associations of the CC watershed have been described in detail in a previous
101 publication (Guedron et al., 2009). Oxisols are developed on the hill tops and on the steep
102 upper- and middle-slopes, ultisols occur mostly on the foot-slopes, and hydromorphic soils

103 are found in the valley referred to as “flats”. A large part of the watershed was considered to
104 be pristine while in the lowland, ancient “Long Tom” sluices, gold-bearing gravel heaps and
105 elemental Hg droplets attest to the former gold-mining activities dating from the early 1950s.
106 **Hydrology:** The Combat Creek is a tributary of the *Boulanger River* (BR). The CC watershed
107 outlet exhibits a permanent discharge, in contrast to intermittent flow in upstream channels.
108 Water discharge response to rain is progressive and lasting, with a high amplitude at the
109 outlet, contrary to upstream and midstream sections, where the response is rapid and short
110 with low amplitude. Surface runoff is visible during heavy rainfalls on the steep hill slopes
111 (often between 15 and 30%). In the former gold mined flat, due to the disorganized original
112 topography, the flow is fractionated into a web of small creek tributaries and multiple
113 stagnant water zones which are not always linked to each other or connected to the
114 hydrographic network.

115 **2.2 Sampling procedure**

116 Four points were monitored along the streams (Fig. 1): PS (pristine spring) is a spring (S) of
117 the CC which drains a small sub-watershed and only flows during the rainy season; MS
118 (middlestream) and CO (contaminated flat outlet) are respectively in the upstream and
119 downstream part of the former gold mined flat; BR is located on the Boulanger River,
120 upstream the confluence with the CC (Fig.1). Rain and stream waters were sampled during
121 and between fourteen rain events at the beginning (08th, 09th and 13th December 2005; 08th,
122 09th and 12^{sd} December 2006) and in the middle of the rainy season (24th, 25th, 27th and 30th
123 May 2005; 18th, 20th, 21st and 25th June 2006). In addition, several superficial stagnant water
124 areas of the former gold mined flat were sampled, as well as the hydromorphic soil’s pore
125 waters. Metacrylate-lined rain gauges were set up close to each sampling point to measure
126 rain fall under forest cover and to collect throughfall samples after each rain event. At the
127 pristine spring, an additional rain gauge was set up outside the forest cover to collect rain

128 samples. The creek flow was gauged using a C2 OTT[®] current meter set, a mobile decameter
129 and vertical ladders, as described by Herschy (1995). Mercury specific fluxes were calculated
130 using discharge and Hg concentration data obtained during and between rain events, and
131 considered the surface area of upstream watersheds.

132 On the CC watershed, soil profiles next to PS, MS and CO were sampled systematically along
133 toposequences (Fig. 1). The toposequences next to the MS and CO reached the gold-mined
134 flats. Soil samples were collected, every 10 or 20 cm depths, down to 1 to 2 meters, using an
135 auger. All soil samples were collected in sterile plastic bags.

136 Water sample collection and treatment were performed using ultra-clean techniques (Cossa et
137 al., 2000). All materials in contact with samples were acid-washed (5 days in 20% HNO₃ v/v,
138 then 3 days in HCl 10 % v/v) and rinsed several times with demineralized water (Milli-Q[®])
139 before use. Polyethylene gloves were used for handling operations. Clean Teflon[®] (FEP)
140 bottles were stored in double polyethylene bags until use. Aliquots for total dissolved mercury
141 ((HgT)_D) and dissolved methylmercury ((MMHg)_D) analysis were collected in FEP bottles
142 and acidified (HCl 0.5 % v/v, Millipore Seastar) after filtration on 22-mm-filters (0.45 μm
143 Sterivex[®]-HV) (Parker et al., 2005). Dissolved Organic Carbon (DOC) samples were stored in
144 Pyrex[®] bottles (previously heated at 500°C) and acidified (HCl 1 % v/v, Millipore Seastar)
145 after filtration (0.45 μm Sterivex[®]-HV). Total particulate mercury ((HgT)_P) and
146 methylmercury ((MMHg)_P) samples were obtained by filtration on 47-mm-diameter filters
147 (0.45 μm hydrophilic - LCR Teflon[®]) (Cossa et al., 1996). All samples for major elements
148 were filtered (0.45 μm PVDF). Samples for cations analysis were acidified (HNO₃ 2 % v/v,
149 Seastar), and samples for anion analysis were stored in polyethylene bottles and frozen until
150 analysis. Particulate Organic Carbon (POC) samples were obtained through filtration (0.7 μm
151 GF/F[®], Whatman).

152 Interstitial soil waters were sampled using Milli-Q[®] rinsed microporous polymer tube
153 samplers (Rhizon[®] SMS, Rhizosphere Research Products). The samplers were placed on the
154 CC bank between the stream sampling points. One interstitial soil water profile was sampled
155 using dialysis membrane techniques (metacrylate peeper) with a 0.45 µm HAWP membrane.
156 The peeper was first acid washed as described above, then filled with Milli-Q[®] water and
157 degassed with Hg-free nitrogen during a 15-day period. The peeper was placed in a
158 hydromorphic soil from the former gold mined flat for 15 days for osmotic equilibration. The
159 Eh profile was monitored several centimeters away from the peeper on the last day of
160 equilibration just before the removal of the peepers. The sulfide-accumulating zone (SAZ)
161 was identified with sulfide-sensitive sellotape (fixed on the peeper), through the formation of
162 a surface darkening Ti-S complex (Jezequel et al., 2007). Aliquots for (MMHg)_D, DOC,
163 anions, sulfides and (Fe^{II}) analysis were sampled in peeper cells every 3 cm and stored as
164 previously described.

165 **2.3 Analytical measurements**

166 **Soil analysis:** Soil samples were freeze-dried, sieved, and the fraction < 2 mm was crushed to
167 grain size smaller than 63 µm for Hg analysis. Total Hg concentrations ([HgT]) were
168 determined by atomic absorption spectrophotometry after dry mineralization and gold
169 amalgamation with an automatic mercury analyser (Altec, Model AMA 254) with a relative
170 precision of ± 10 % (Roos-Barracough et al., 2002). Concentrations obtained for repeated
171 analyses of certified reference materials (CRM) never exceeded the range of concentration
172 given for standards CRM 7002 (0.09 ± 0.012 µg g⁻¹ - Czech Metrological Institute) and
173 MESS-3 (0.091 ± 0.008 µg g⁻¹ - National Research Council of Canada). The analytical quality
174 was assured by analyzing every sample twice. Typically, the measurement error is usually
175 about 5% and always below 10%. The detection limit, defined as three times the standard
176 deviation of the blank (SD_{blk}), was 0.005 µg g⁻¹.

177 **Water analyses:** Samples were analysed for [(HgT)_D] and [(HgT)_P], [(MMHg)_D] and
178 [(MMHg)_P] by cold vapor atomic fluorescence spectrometry (CVAFS) after conversion of all
179 mercury species into Hg⁰ (Bloom et al., 1988) followed by detection using a Tekran[®] (Model
180 2500) mercury detector. The principles of the methods used originate from the Bloom and
181 Fitzgerald (1988) gold amalgamation method for (HgT)_D, from the Liang et al. (1994)
182 ethylation method for (MMHg)_P and from the Tseng et al. (1998) hydruation method for
183 (MMHg)_D modified by Cossa et al. (2009). (HgT)_P was performed after HCl/HNO₃ digestion
184 (10h at 70°C) in PFA Teflon reactors (Coquery et al., 1997). The detailed procedures are
185 described elsewhere (Cossa et al., 2003, Cossa et al., 2002). These quantifications were
186 performed after checking for possible interference with the internal spikes (Coquery et al.,
187 2003). The accuracy of analyses was checked using the CRM ORMS-3 (National Research
188 Council of Canada) for (HgT)_D, CRM 7002 for (HgT)_P and CRM ERM-AE670 (IRMM -
189 European Commission) for (MMHg)_D and (MMHg)_P. Analytical quality was assured by
190 triplicating several samples, and the measurement error usually was approximately 10 % and
191 always below 15% for [(HgT)_D], [(HgT)_P], and [(MMHg)_D] and always below 30 % for
192 [(MMHg)_P]. The detection limits (3SD_{blk}) were 0.01 ng L⁻¹ for (HgT)_D, 0.004 ng L⁻¹ for
193 (MMHg)_D, and 0.05 ng g⁻¹ for (MMHg)_P. Dissolved chloride, sulfate and nitrate ([Cl⁻], [SO₄²⁻]
194 and [NO₃⁻]) were determined using ionic chromatography (Dionex, model CD20). Dissolved
195 reduced iron ([Fe^{II}]) and sulfide ([S^{II}]) were measured in the field with a Hach[®] (model
196 DR/850) spectrometer (methods 8146 and 8131 for [Fe^{II}] and [S^{II}], respectively). [DOC] was
197 determined using a Non Dispersive Infra-Red CO₂ spectrometer (NDIR, Shimatzu[®]) after
198 humid oxidation in a sodium persulfate solution at 100°C. [POC] was determined by dry
199 combustion of GF/F filters, using a Fisons 1500 CHN autoanalyser. Detection limits (3SD_{blk})
200 were 0.06 and 0.05 mg L⁻¹ for [SO₄²⁻] and [NO₃⁻], 0.01 mg L⁻¹ for [Fe^{II}] and [S^{II}], and 0.2 mg
201 L⁻¹ for [DOC]). Eh, pH and conductivity were performed in situ using a Sentron Eh meter

202 (model, Argus with probe 67597), a WTW pH meter and a conductimeter (model 340i),
203 respectively.

204 **2.4 Use of chloride as hydrological index**

205 Chloride (Cl^-) was used as a hydrological index to trace the proportion of mixing in the stream
206 between recent water, generally surface runoff characterized by low $[\text{Cl}^-]$ close to throughfall
207 concentrations, and old water, corresponding to subsurface runoff or deep groundwater with
208 typically higher $[\text{Cl}^-]$ (Christophersen et al., 1990, Grimaldi et al., 2004, Peters et al., 1998,
209 Soulsby et al., 2007). The $[\text{Cl}^-]$ increase between both hydrological compartments is due to
210 evapo-transpiration related to the residence time of water in the soil. Cl^- was thus used as a
211 conservative element to compare the behaviour of the various Hg species.

212 **2.5 Statistical treatment**

213 Since most geochemical data were not normally distributed, we have listed in tables: the
214 mean, the median and the standard error of the mean (SEM), and as suggested by Webster
215 (2001), the 6 following parameters (supplementary data): the mean, the standard error of the
216 mean (SEM), the median, 25th percentiles (25th perc.), 75th percentiles (75th perc.) and the
217 number of observations (N). We also used non-parametric tests, the Mann-Whitney rank sum
218 test (U test), or the Kruskal-Wallis one way analysis of variance on ranks (H test), to compare
219 two, or more than two sets of data, respectively, and pairwise multiple comparison according
220 to Dunn's method to isolate the set or sets that differed from the others. Correlation
221 coefficients (R) and P values (P) are reported. All statistical analyses were performed using
222 Sigmastat[®].

223

224 **3. Results**

225 **3.1 Total Hg in soils**

226 On the slopes of the pristine part of the watershed, soil [HgT] globally decreased from oxisols
227 to ultisols (Tab. 1), but the difference was statistically significant (*t* test, $P < 0.001$) only for
228 the deeper layers ($> 0.5\text{m}$), because [HgT] rapidly decreased with depth in the ultisols. Soil
229 surface layer [HgT] significantly increased (*U* Test, $P=0.006$) from the pristine to the former
230 gold mine flat soils (by a factor between 2 and 4 for the median values), up to a [HgT]
231 maxima of $5.47 \mu\text{g g}^{-1}$. [HgT] were highly variable over short distances and with depth in the
232 former gold mined flat.

233

234 **3.2 Total Hg in stream and rain waters**

235 A global increase in total Hg concentrations (Tab. 2) in the CC stream waters was observed
236 between the pristine spring (PS) and the contaminated flat outlet (CO). $[(\text{HgT})_P]$ and $[(\text{HgT})_D]$
237 significantly increased downstream (*H* test, $P < 0.001$) from PS to CO. On the contrary
238 $[(\text{HgT})_P]$ and $[(\text{HgT})_D]$ were not significantly different between CO and BR. $[(\text{HgT})_D]$ were
239 higher in both throughfall and rain waters than in stream waters at PS and MS (*U* test,
240 $P < 0.001$), and were in the range of $[(\text{HgT})_D]$ measured at (Tab. 2 and 3 and Fig. 2).
241 Conversely, $[\text{Cl}^-]$ were higher in stream waters at PS than in throughfall and rain waters (*H*
242 test, $P < 0.001$) due to the residence time in soil. Downstream, $[\text{Cl}^-]$ increased at CO, fed by
243 older waters than the outlet of the pristine sub-catchment.

244 Most of the total Hg measured in the stream was bound to suspended particles with log
245 partitioning coefficients ($\log K_D = \log[(\text{HgT})_P] - \log[(\text{HgT})_D]$) ranging from 3.8 to 8.3, with a
246 median value of 5.9. HgT was not specifically associated with suspended organic particles
247 since no correlation was observed between $[(\text{HgT})_P]$ and [POC].

248 Seasonal variations for total Hg concentrations were noticeable at MS and CO. At PS, the
249 absence of discharge at the beginning of the rainy season precluded water sampling and
250 seasonal comparison. $[(\text{HgT})_P]$ at CO were lower during the rain events at the beginning of

251 the rainy season than those in the middle (*U* test, $P < 0.05$; respective medians of 1.01 and
252 $0.77 \mu\text{g g}^{-1}$). $[(\text{HgT})_{\text{D}}]$ at MS and CO were higher at the beginning of the rainy season than
253 later in the season (*U* test, $P < 0.05$) (Fig. 2). At the same time, $[\text{Cl}^-]$ decreased between the
254 beginning and the middle of the rainy season (*U* test, $P < 0.05$) due to the progressive renewal
255 of soil waters and/or to the increase of surface water runoff in relation with intense rain events
256 and to soil water saturation.

257

258 **3.3 Methylmercury in stream and rain waters**

259 The mean $[\text{MMHg}]/[\text{HgT}]$ ratios in stream waters equalled 2 % and 1 %, for the particulate
260 and dissolved phases, respectively. For total Hg, a large downstream increase was observed
261 for MMHg concentrations between the pristine sub-watershed and the contaminated flat (Tab.
262 2). $[(\text{MMHg})_{\text{P}}]$ were similar at PS, MS and BR but higher at CO (*H* test, $P < 0.001$), with a 3
263 times median increase between PS and CO. $[(\text{MMHg})_{\text{D}}]$ measured at PS and MS were very
264 low, often under the detection limit ($< 0.004 \text{ ng L}^{-1}$), but significantly increased at CO (*H* test,
265 $P < 0.001$), with a high variability. $[(\text{MMHg})_{\text{D}}]$ at BR ranged between the concentrations
266 measured at PS, MS, and CO. In rain samples, $[(\text{MMHg})_{\text{D}}]$ were not significantly different
267 than those in throughfalls, however, both were a slightly larger than the concentrations
268 measured in PS stream waters (Tab. 3).

269 MMHg had a strong affinity for particulate organic matter since log partitioning coefficients
270 ($\log K_{\text{D}} = \log[(\text{MMHg})_{\text{P}}] - \log[(\text{MMHg})_{\text{D}}]$) were high (between 7.4 and 9.5), and $[(\text{MMHg})_{\text{P}}]$
271 measured at CO were correlated with [POC] ($R = 0.457$, $P < 0.05$, $N = 24$). $[(\text{MMHg})_{\text{P}}]$
272 monitored at CO were lower at the beginning than in the middle of the rainy season (*U* test,
273 $P < 0.001$; respective medians of 12.26 and 5.59 ng g^{-1}), as opposed to $[(\text{MMHg})_{\text{D}}]$ which was
274 highly variable but globally higher (*U* test, $P < 0.001$) at the beginning of the rainy season than
275 in the middle.

276

277 **3.4 Dissolved total and methyl mercury in soil waters of the gold mined flat**

278 [(MMHg)_D] measured in various locations of the former gold mined flat area largely exceeded
279 those measured in the pristine area for both overlying and subsurface soil pore waters (Tab. 3,
280 Fig. 3). The highest [(MMHg)_D] were related to slightly negative or positive Eh values and
281 high [Fe^{II}]. They also were associated with pH values between 5 and 6, while pH values
282 measured in stream waters ranged from 4 to 5. High [(HgT)_D] also were found in these soil
283 waters, especially with low Eh conditions and high [Fe^{II}] (Fig. 3); however, no relation was
284 observed between [(HgT)_D] and [(MMHg)_D].

285 Figure 4 illustrates a complete vertical profile of [(MMHg)_D] for both overlying and pore
286 waters of a disorganized hydromorphic soil of the flat, sampled near an ancient sluice at the
287 beginning of the rainy season. In this profile, [(MMHg)_D] were low in the pore water and
288 sharply increased in the overlying water. High [(MMHg)_D] were found in the upper part of the
289 SAZ where the Eh increased, and above the SAZ where [Fe^{II}] sharply increased.

290 Both median [(MMHg)_D] and [(HgT)_D] in overlying soil and pore waters were higher at the
291 beginning of the rainy season (0.27 ng L⁻¹ and 4.27 ng L⁻¹, for (MMHg)_D and (HgT)_D,
292 respectively) than in the middle of the rainy season (0.11 ng L⁻¹ and 1.60 ng L⁻¹, for
293 (MMHg)_D and (HgT)_D, respectively - *H* test, *P*<0.01).

294

295 **4. Discussion**

296 **4.1 Oxisols as a sink of total mercury and methylmercury in the pristine area**

297 In the pristine area of the CC watershed, the decreasing [(HgT)_D] with increasing [Cl⁻] found
298 between rain or throughfall waters and the stream (Fig. 2) is due to the adsorption of Hg on
299 oxisol components during water percolation. The strong adsorption capacity of oxisols

300 already was observed in another study on the Hg distribution in oxisols at the same site
301 (Guedron et al., 2009).

302 The comparison of our data with those of other studies showed that in rain and throughfall
303 waters, [(HgT)_D] were within the range of reported concentrations for 83 rain events ($2.34 \pm$
304 0.27 ng L^{-1}) monitored in French Guiana (Muresan et al., 2007b) and that [(MMHg)_D] were
305 within the range of concentrations published for temperate regions (Lawson et al., 2001) and
306 for 50 rain events ($0.03 \pm 0.09 \text{ ng L}^{-1}$) monitored in French Guiana (Muresan et al., 2007b). In
307 spring waters, [(HgT)_D] were similar to concentrations reported for larger Amazonian rivers
308 (0.4 to 2.8 ng L^{-1} in Lechler et al., 2000, Roulet et al., 1998a) and [(MMHg)_D] were within the
309 range of concentrations reported by several authors (Bisinoti et al., 2007, Roulet et al., 1999a)
310 for large Amazonian rivers (0.02 to 0.24 ng L^{-1}) and for large French Guiana rivers (0.06 - 0.10
311 ng L^{-1} according to Muresan, 2006, Roulet et al., 1999a). These comparisons confirm that
312 tropical soils act as a sink for Hg and regulate Hg fluxes towards small as well as large
313 hydrosystems (Roulet et al., 2001).

314

315 **4.2 Evidence of soil total mercury contamination in the former gold mined flat**

316 The [(HgT)] reaching up to 100 times the values reported from pristine hydromorphic soils in
317 French Guiana (Guedron et al., 2006) demonstrates the large contamination of the former
318 gold mined flat by mercury. This large Hg contamination of the flat explains the downstream
319 increase of [(HgT)_P] along the stream (Tab. 2), which carries an increased proportion of
320 contaminated particles from the pristine spring to the flat outlet. [(HgT)_P] in suspended
321 particles are higher than in the soil surface (Tab. 1 and 2), since suspended particles consist of
322 the soil's finest granulometric fraction, which are enriched in Hg (Grimaldi et al., 2008). In
323 contrast, [(HgT)_P] monitored at the outlet of the pristine sub-catchment are within a similar

324 range of reported data from larger Amazonian rivers (0.11 to 0.36 $\mu\text{g g}^{-1}$ in Lechler et al.,
325 2000, Roulet et al., 1998a).

326

327 **4.3 Hydromorphic soils as a source of methyl mercury for the stream**

328 While the downstream increase in $[(\text{HgT})_{\text{P}}]$ and $[(\text{HgT})_{\text{D}}]$ is gradual until reaching the
329 watershed outlet, the sharp increase in $[(\text{MMHg})_{\text{P}}]$ and $[(\text{MMHg})_{\text{D}}]$ between MS and CO
330 suggests a particularly strong MMHg input from the contaminated flat. Both $[(\text{MMHg})_{\text{P}}]$ and
331 $[(\text{MMHg})_{\text{D}}]$ monitored at the outlet of the watershed exceeded the range of concentrations
332 given in the literature cited above for large Amazonian and French Guiana rivers, including
333 the Boulanger river (Muresan, 2006, Roulet et al., 1999a). Puddles and pore waters of
334 hydromorphic soils are the most probable MMHg sources in the flat.

335 The numerous locally isolated water puddles in the flat are attributed to former mining
336 activities which have strongly disturbed the flat's topography. The former "Long Tom"
337 mining process and stream tapping, which was shifted laterally by miners along the flat, have
338 led to a web of small creek tributaries and to multiple stagnant water areas which are not
339 always connected to the hydrographical network. The intense disturbance of soil structure
340 leads to local drainage deficiency reflected by the presence of quasi-permanently flooded
341 soils. Because the ancient gold-mining activities, such as gold amalgamation and burning of
342 amalgams, were performed on site, Hg contamination in the flat is due both to the loss of Hg^0
343 droplets, and to the rapid deposition of atmospheric Hg in the local environment. This
344 explains the high variability of $[\text{HgT}]$ in soils. In addition, Hg was observed to be present
345 mainly in its elemental form in these contaminated soils (Guedron et al., 2009). The high
346 $[(\text{MMHg})_{\text{D}}]$ monitored in various locations of the flat corroborates the laboratory simulation
347 of gold-mining activities (Dominique et al., 2007), which indicated that the presence of Hg^0
348 can enhance Hg methylation in the Amazonian environment. The local soil disturbance

349 favours the existence of high methylation areas. In hydromorphic soils and isolated puddles,
350 water residence time can be long, which induces anoxic conditions and high concentrations of
351 dissolved elements. Low Eh, pH between 5 and 6, iron oxides, high concentrations of DOC,
352 SO_4^{2-} and $(\text{HgT})_{\text{D}}$ are favorable for methylation (Benoit et al., 1999, Benoit et al., 2003,
353 Bisogni et al., 1975, Mason et al., 1995). Under these conditions iron-reducing as well as
354 sulfate-reducing bacteria (IRB and SRB, respectively) are reported to be the main mercury
355 methylators (Barkay et al., 1997, Fleming et al., 2006). The increase of $[(\text{MMHg})_{\text{D}}]$ within the
356 10 first centimetres of overlying waters with high dissolved $[\text{Fe}^{\text{II}}]$, and to a lesser extent in the
357 upper SAZ in soil pore waters (Fig. 4) reinforces the hypothesis of a contribution of IRB and
358 SRB in the methylation, as supported by archetypal chemical changes where microorganisms
359 shift from $\text{FeOOH}(\text{s})$ to SO_4^{2-} as an electron acceptor. The occurrence of high $[(\text{MMHg})_{\text{D}}]$
360 with high $[\text{Fe}^{\text{II}}]$ suggests a greater availability of $(\text{HgT})_{\text{D}}$ for IRB than for SRB in the SAZ,
361 since in absence of sulfides, the adsorption and co-precipitation of $\text{Hg}(\text{II})$ onto $\text{FeS}(\text{s})$ is
362 restricted (Fink, 2002, Mehrotra et al., 2003, Mehrotra et al., 2005). The striking feature of
363 high $[(\text{MMHg})_{\text{D}}]$, associated with slightly negative or slightly positive Eh values measured in
364 various overlying and soil pore waters of the flat (Fig. 3 and 4), corresponds well with the
365 observations made in lake sediment/water interfaces (Birkett et al., 2005, Muresan et al.,
366 2007a, Muresan et al., 2007b, Ullrich et al., 2001).

367

368 **4.4 Seasonal influence on MMHg emissions to the stream.**

369 The favourable geochemical conditions for mercury methylation can occur during the dry
370 season when they are favoured by a long residence time of water in puddles and soils of the
371 gold mined flat. At the beginning of the rainy season $(\text{MMHg})_{\text{D}}$ is discharged by pulses
372 during rain events which leads to high concentrations in the stream. In the middle of the rainy
373 season the decrease of $[(\text{MMHg})_{\text{D}}]$ is due both to unfavourable methylation conditions and

374 global dilution, as indicated by $[Cl^-]$ decrease at the same time. Similarly, the gold mined flat
375 puddles and soil pore waters are more concentrated in Cl^- at the beginning of the rainy season
376 than later (*U* test, $P < 0.05$). As for Cl^- , the renewal of stagnant overlying and pore waters of
377 the contaminated flat leads to the dilution of $(MMHg)_D$ and $(HgT)_D$, as well as other dissolved
378 elements such as DOC and SO_4^{2-} . The dissolution of particulate OM and minerals, as well as
379 methylation reactions are slow reactions (Bisogni et al., 1975, Langley, 1973). Therefore,
380 since DOC is the most important complexing ligand in surface waters in the absence of
381 sulphide the bio-availability of Hg for methylating bacteria may decrease in the middle of the
382 rainy season (Benoit et al., 2003, Ullrich et al., 2001). The change in geochemical conditions
383 such as the decrease of pH and conductivity and the increase in Eh from the beginning to the
384 middle of the rainy season, also limits bacterial activity and Hg availability, which can lead to
385 the decrease of methylation rates (Birkett et al., 2005, Ullrich et al., 2001).

386

387 **4.5 Hg and MMHg export from the CC watershed to the stream**

388 The comparison of (HgT) and $(MMHg)$ specific fluxes between the outlet of the pristine
389 oxisol sub-watershed (PS) and the entire watershed (CO) indicates that the contribution of the
390 contaminated flat is especially substantial for $(MMHg)$. Additionally, calculated specific
391 fluxes for both dissolved and particulate $MMHg$ were increased by factors of 6 and 4 between
392 PS and CO, respectively (*U* tests, $P \leq 0.001$ - Tab. 4), while those for $(HgT)_D$ and $(HgT)_P$ were
393 within the same range and doubled (*U* test, $P = 0.043$) between PS and CO, respectively. The
394 estimation of annual specific fluxes from the CC watershed highlights its large contamination,
395 all the more since the flat's contribution is diluted by the fluxes originating from the pristine
396 soils which cover the majority of the watershed and act as a sink for Hg and $MMHg$.
397 The comparison of our data with calculated fluxes in other Amazonian locations corroborates
398 this point. For example, the annual $(HgT)_P$ export at the outlet of the CC watershed (mean =

399 $93 \pm 37 \mu\text{g m}^{-2} \text{yr}^{-1}$) is much larger than the fluxes ($2.6 - 8.5 \mu\text{g m}^{-2} \text{yr}^{-1}$) calculated for a small
400 forested Amazonian area (1.6 km^2), located far from gold-mining activities (Fostier et al.,
401 2000), and for fluxes ($30 \text{ to } 35 \mu\text{g m}^{-2} \text{yr}^{-1}$) measured for the large Cururai floodplain system
402 (Maia et al., 2009) where the large size of the basin (3800 km^2) may dilute the fluxes
403 originating from gold mined areas significantly. Our data also exceed the range of fluxes
404 found for the Seine river (Coquery et al., 1997) and for urban-type watersheds ($0.2 - 20 \mu\text{g m}^{-2}$
405 yr^{-1}) according to the Wisconsin's US system of rivers classification (Hurley et al., 1995).
406 No MMHg fluxes are available for Amazonian watersheds. However, a comparison with
407 boreal and temperate environments shows that the $(\text{MMHg})_{\text{P}}$ exported from the CC watershed
408 (mean fluxes = $0.68 \pm 0.12 \mu\text{g m}^{-2} \text{yr}^{-1}$) is larger compared to fluxes ($0.02 \text{ to } 0.183 \mu\text{g m}^{-2} \text{yr}^{-1}$)
409 measured for a selection of sixteen US streams (Balogh et al., 2005, Brigham et al., 2009).

410

411 **5. Conclusions**

412 This study shows that, even 60 years after exploitation, former gold-mining activities largely
413 contribute to the in-stream load of MMHg, whereas their contribution for total mercury
414 remains moderated. Hydromorphic soils, disturbed and strongly Hg contaminated (including
415 Hg^0 droplets) by former gold-mining, were identified as the main sources of MMHg.
416 Methylation was suggested to be induced mainly by IRB during the dry season when the
417 surface and pore waters are stagnant, whereas emissions of MMHg occurred during rainy
418 season events when these waters are discharged into the stream.

419 Such former goldmines can still contribute to MMHg inputs in larger hydrological systems.
420 Numerous former and current artisanal or semi-industrial goldmines exist in French Guiana
421 and elsewhere in Amazonia, but these areas are rarely mapped or referenced. Thus, the
422 evaluation of the real contribution of these former activities is sorely quantifiable and
423 suggests that it is an important contributor of MMHg emissions in Amazonian hydrosystems.

424 The continuous expansion of legal and illegal gold-mining in French Guiana implies an
425 increase in dissolved and particulate MMHg emissions in the hydrographic network, with an
426 enhancement of MMHg contamination of aquatic ecosystems and the consequent increase in
427 the toxicological threat for local human populations whose diet relies mainly on fish.

428

429 **Acknowledgments**

430 This research was supported mainly by the CNRS, FNS, FEDER, MATE/DIREN, and ANR
431 as a part of the Mercury in French Guiana research program and by the Boulanger Mine
432 Company (CMB). We acknowledge Jennifer Harris-Hellal, Nouredine Bousserhine, Genlis
433 Gallifet and Dennis Lahondes for additional support on this project. We also, acknowledge
434 Bernard Averty from the IFREMER Laboratory of Nantes for support in methylmercury
435 analysis.

436

437 **References**

438

- 439 Balogh, S.J., Nollet, Y.H. and Offerman, H.J. (2005) A comparison of total mercury and
440 methylmercury export from various Minnesota watersheds. *Sci. Tot. Environ.* 340(1-3),
441 261-270.
- 442 Barbosa, A.C., Souza, J.d., Dorea, J.G., Jardim, W.F. and Fadini, P.S. (2003) Mercury
443 Biomagnification in a Tropical Black Water, Rio Negro, Brazil. *Arch. Environ. Contam.*
444 *Toxicol.* 45(2), 235-246.
- 445 Barkay, T., Gillman, M. and Turner, R. (1997) Effects of dissolved organic carbon and
446 salinity on bioavailability of mercury. *Appl. Environ. Microbiol.* 63(11), 4267-4271.
- 447 Barret, J. (2004) *Illustrated Atlas of French Guyana* (in French), French Guyana Publications,
448 Cayenne.
- 449 Benoit, J., Gilmour, C., Mason, R. and Heyes, A. (1999) Sulfide controls on mercury
450 speciation and bioavailability to methylating bacteria in sediment pore waters. *Environ.*
451 *Sci. Technol.* 33, 951-957.
- 452 Benoit, J.M., Gilmour, C.C., Heyes, A., Mason, R.P. and Miller, C.L. (2003)
453 Biogeochemistry of Environmentally Important Trace Elements. Cai, Y. and Braids,
454 O.C. (eds), pp. 262-297, Oxford University Press.
- 455 Birkett, J. and Lester, J. (2005) Distribution of mercury and methylmercury in the sediments
456 of a lowland river system. *Proceedings of the Royal Society A: Math., Phys. Eng. Sci.*
457 461(2057), 1335-1355.
- 458 Bisinoti, M.C., Sargentini Júnior, E. and Jardim, W.F. (2007) Seasonal Behavior of
459 Mercury Species in Waters and Sediments from the Negro River Basin, Amazon,
460 Brazil. *J. Braz. Chem. Soc.* 18(3), 544-553.
- 461 Bisogni, J.J. and Lawrence, A.W. (1975) Kinetics of mercury methylation in aerobic and
462 anaerobic aquatic environments. *J. Water Pollut. Control Fed.* 47(1), 135-152.
- 463 Bloom, N.S. and Fitzgerald, W.F. (1988) Determination of volatile mercury species at the
464 picogram level by low-temperature gas chromatography with cold-vapor atomic
465 fluorescence detection. *Anal. Chim. Acta* 208, 151-161.
- 466 Brabo, E.D., Santos, E.D., de Jesus, I.M., Mascarenhas, A.F.S. and Faial, K.D. (2000)
467 Mercury contamination of fish and exposures of an indigenous community in Para
468 State, Brazil. *Environ. Res.* 84(3), 197-203.
- 469 Brigham, M.E., Wentz, D.A., Aiken, G.R. and Krabbenhoft, D.P. (2009) Mercury Cycling in
470 Stream Ecosystems. 1. Water Column Chemistry and Transport. *Environ. Sci. Technol.*
471 43(8), 2720-2725.
- 472 Christophersen, N. and Neal, C. (1990) Linking hydrological, geochemical, and soil chemical
473 processes on the catchment scale: an interplay between modelling and field work. *Water*
474 *Resour. Res.* 26, 3077-3086.
- 475 Coquery, M., Cossa, D., Azemard, S., Peretyazhko, T. and Charlet, L. (2003) Methylmercury
476 formation in the anoxic waters of the Petit-Saut reservoir (French Guiana) and its
477 spreading in the adjacent Sinnamary river. *J. Phys. IV* 107, 327-331.
- 478 Coquery, M., Cossa, D. and Sanjuan, J. (1997) Speciation and sorption of mercury in two
479 macro-tidal estuaries. *Mar. Chem.* 58(1-2), 213-227.
- 480 Cossa, D., Averty, B., Bretaudeau, J. and Senard, A.S. (2003) Dissolved mercury speciation
481 in marine waters. *Analysis methods in marine environment, Ifremer and French*
482 *Ecology, Durable Development Ministry* (in French).
- 483 Cossa, D., Averty, B. and Pirrone, N. (2009) The origin of methylmercury in open
484 Mediterranean waters. *Limnol. Oceanogr.* 54(3), 837-844.

- 485 Cossa, D., Coquery, M., Gobeil, C. and Martin, J. (1996) Regional and Global Cycles of
486 Mercury: Sources, Fluxes, and Mass Balances. Baeyens, W., Ebinghaus, R. and
487 Vasiliev, O. (eds), pp. 229-247, Kluwer Academic Publishers, Dordrecht, The
488 Netherlands.
- 489 Cossa, D., Coquery, M., Nakhle, K. and Claisse, D. (2002) Total mercury and
490 monomethylmercury analysis in marine organisms and sediments. Analysis methods in
491 marine environment, Ifremer and French Ecology, Durable Development Ministry (in
492 French).
- 493 Cossa, D. and Gobeil, C. (2000) Mercury speciation in the Lower St. Lawrence estuary. *Can.*
494 *J. Fish. Aquat. Sci.* 57, 138-147.
- 495 Dominique, Y., Muresan, B., Duran, R., Richard, S. and Boudou, A. (2007) Simulation of the
496 Chemical Fate and Bioavailability of Liquid Elemental Mercury Drops from Gold
497 Mining in Amazonian Freshwater Systems. *Environ. Sci. Tech.* 41(21), 7322 -7329.
- 498 Dorea, J.G. and Barbosa, A.C. (2007) Anthropogenic impact of mercury accumulation in fish
499 from the Rio Madeira and Rio Negro rivers (Amazonia). *Biol. Trace Element Res.*
500 115(3), 243-254.
- 501 Durrieu, G., Maury-Brachet, R. and Boudou, A. (2005) Goldmining and mercury
502 contamination of the piscivorous fish, *Hoplias aimara* in French Guiana (Amazon
503 basin). *Ecotoxicol. Environ. Saf.* 60(3), 315-323.
- 504 Fink, L. (2002) Status Report on the Effect of Water Quantity and Quality on Methylmercury
505 Production, pp. 2B2.1-2B2.17, EPA.
- 506 Fleming, E.J., Mack, E.E., Green, P.G. and Douglas, C.N. (2006) Mercury methylation from
507 unexpected sources :molybdate-inhibited freshwater sediments and iron-reducing
508 bacterium. *Appl. Environ. Microbiol.* 72(1), 457-464.
- 509 Fostier, A.-H., Forti, M.c., Guimaraes, J.R.D., Melfi, A.J., Boulet, R., Espirito Santo, C.M.
510 and Krug, F.J. (2000) Mercury fluxes in a natural forested Amazonian catchment (Serra
511 do Navio, Amapa State, Brazil). *Sci. Tot. Environ.* 260, 201-211.
- 512 Frery, N., Maury-Brachet, R., Maillot, E., Deheeger, M., Merona de, B. and Boudou, A.
513 (2001) Goldmining activities and mercury contamination of native Amerindian
514 communities in french Guiana: key role of fish in dietary uptake. *Environ. Health Persp.*
515 109(5), 449-456.
- 516 Grimaldi, C., Grimaldi, M. and Guédron, S. (2008) Mercury distribution in tropical soil
517 profiles related to origin of mercury and soil processes. *Sci. Total Environ.* 401, 121-
518 129.
- 519 Grimaldi, C., Grimaldi, M., Millet, A., Bariac, T. and Boulègue, J. (2004) Behavior of
520 chemical solutes during a storm in a rainforested headwater catchment. *Hydrol. Process.*
521 18, 93-106.
- 522 Guedron, S., Grangeons, S., Lanson, B. and Grimaldi, M. (2009) Mercury speciation in a
523 tropical soil association; Consequence of gold mining on Hg distribution in French
524 Guiana. *Geoderma* 153, 331-346.
- 525 Guedron, S., Grimaldi, C., Chauvel, C., Spadini, C. and Grimaldi, M. (2006) Weathering
526 versus atmospheric contributions to mercury concentrations in French Guiana soils.
527 *Appl. Geochem.* 21, 2010-2022.
- 528 Hall, B.D., Aiken, G.R., Krabbenhoft, D.P., Marvin-DiPasquale, M. and Swarzenski, C.M.
529 (2008) Wetlands as principal zones of methylmercury production in southern Louisiana
530 and the Gulf of Mexico region. *Environ. Pollut.* 154(1), 124-134.
- 531 Harper, B.L. and Harris, S.G. (2008) A possible approach for setting a mercury risk-based
532 action level based on tribal fish ingestion rates. *Environ. Res.* 107(1), 60-68.
- 533 Herschy, R.W. (1995) *Streamflow Measurement*, Elsevier Applied Science.

- 534 Hurley, J.P., Benoit, J.M., Babiarz, C.L., Shafer, M.M., Andren, A.W., Sullivan, J.R.,
535 Hammond, R. and Webb, D.A. (1995) Influence of watershed characteristics on
536 mercury levels in Wisconsin rivers. *Environ. Sci. Technol.* 29(7), 1867-1875.
- 537 Jezequel, D., Brayner, R., Metzger, E., Viollier, E., Prevot, F. and Fievet, F. (2007) Two-
538 dimensional determination of dissolved iron and sulfur species in marine sediment pore-
539 waters by thin-film based imaging. Thau lagoon (France). *Estuarine Coastal Shelf Sci.*
540 72(3), 420-431.
- 541 Lambertsson, L. and Nilsson, M. (2006) Organic Material: The Primary Control on Mercury
542 Methylation and Ambient Methyl Mercury Concentrations in Estuarine Sediments.
543 *Environ. Sci. Technol.* 40(6), 1822-1829.
- 544 Langley, D.G. (1973) Mercury methylation in an aquatic environment. *J. Water Pollut.*
545 *Control Fed.* 45(1), 44-51.
- 546 Lawson, N.M. and Mason, R.P. (2001) Concentration of Mercury, Methylmercury, Cadmium,
547 Lead, Arsenic, and Selenium in the Rain and Stream Water of Two Contrasting
548 Watersheds in Western Maryland. *Water Res.* 35(17), 4039-4052.
- 549 Lechler, P.J., Miller, J.R., Lacerda, L.D., Vinson, D., Bonzongo, J.-C., Lyons, W.B. and
550 Warwick, J.J. (2000) Elevated mercury concentrations in soils, sediments, water, and
551 fish of the Madeira River basin, Brazilian Amazon: a function of natural enrichments?
552 *Sci. Total Environ.* 260, 87-96.
- 553 Liang, L., Bloom, N.S. and Horvat, M. (1994) Simultaneous determination of Mercury
554 speciation in biological materials by GC/CVAFS after ethylation and room-temperature
555 precollection. *Clin. Chem.* 40(4), 602-607.
- 556 Maia, P.D., Maurice, L., Tessier, E., Amouroux, D., Cossa, D., Pérez, M., Moreira-Turcq, P.
557 and Rhéault, I. (2009) Mercury distribution and exchanges between the Amazon River
558 and connected floodplain lakes. *Sci. Tot. Environ.* 407, 6073-6084.
- 559 Malm, O. (1998) Gold mining as a source of mercury exposure in the Brazilian Amazon.
560 *Environ. Res.* 77(2), 73-78.
- 561 Marchand, C., Lallier-Verges, E., Baltzer, F., Alberic, P., Cossa, D. and Baillif, P. (2006)
562 Heavy metals distribution in mangrove sediments along the mobile coastline of French
563 Guiana. *Mar. Chem.* 98(1), 1-17.
- 564 Mason, R.P., Reinfelder, J.R. and Morel, F.M.M. (1995) Bioaccumulation of mercury and
565 methylmercury. *Water Air Soil Pollut.* 80, 915-921.
- 566 Mehrotra, A.S., Horne, A.J. and Sedlak, D.L. (2003) Reduction of Net Mercury Methylation
567 by Iron in *Desulfobulbus propionicus* (1pr3) Cultures: Implications for Engineered
568 Wetlands. *Environ. Sci. Technol.* 37(13), 3018-3023.
- 569 Mehrotra, A.S. and Sedlak, D.L. (2005) Decrease in Net Mercury Methylation Rates
570 Following Iron Amendment to Anoxic Wetland Sediment Slurries. *Environ. Sci.*
571 *Technol.* 39(8), 2564-2570.
- 572 Milési, J.P., Egal, E., Ledru, P., Vernhet, Y., Thiéblemont, D., Cocherie, A., Tegye, M.,
573 Martel-Jantin, B. and Lagny, P. (1995) Mineralizations of the northern French Guiana in
574 their geological setting. *Mining Res. Chron.* 518, 5-58 (in French).
- 575 Muresan, B. (2006) Mercury geochemistry in the *continuum of* Petit Saut reservoir and the
576 Sinnamary estuary, French Guiana (in French). P.H.D, University of Bordeaux I, PhD
577 Thesis.
- 578 Muresan, B., Cossa, D., Jezequel, D., Prevot, F. and Kerbellec, S. (2007a) The
579 biogeochemistry of mercury at the sediment-water interface in the Thau lagoon. 1.
580 Partition and speciation. *Estuarine Coastal Shelf Sci.* 72(3), 472-484.
- 581 Muresan, B., Cossa, D., Richard, S. and Burban, D. (2007b) Mercury speciation exchanges at
582 the air-water interface of a tropical artificial reservoir, french guiana. *Sci. Total Environ.*
583 385(1-3), 132-145.

584 Parker, J.L. and Bloom, N.S. (2005) Preservation and storage techniques for low-level
585 aqueous mercury speciation. *Sci. Total Environ.* 337(1-3), 253-263.

586 Peters, N. and Ratcliffe, E. (1998) Tracing hydrologic pathways using chloride at the Panola
587 mountain research watershed, Georgia, USA. *Water Air Soil Poll.* 105, 263-275.

588 Pfeiffer, W.C., Lacerda, L.D., Salomon, W. and Malm, O. (1993) Environmental fate of
589 mercury from gold mining in the Brazilian Amazon. *Environ. Rev.* 1, 26-37.

590 Porvari, P. (1995) Mercury levels of fish in Tucuruí hydroelectric reservoir and in River Moju
591 in Amazonia, in the state of Para, Brazil. *Sci. Total Environ.* 175(2), 109-117.

592 Roos-Barracough, F., Givélet, N., Martínez-Cortizas, A., Goodsite, M.E., Biester, H. and
593 Shoty, W. (2002) An analytical protocol for determination of total mercury
594 concentration in solid peat samples. *Sci. Tot. Environ.* 292, 129-139.

595 Roulet, M., Lucotte, M., Canuel, R., Farella, N., Freitas Goch, Y.G.D., Pacheco Peleja, J.R.,
596 Guimaraes, J.-R.D., Mergler, D. and Amorim, M. (2001) Spatio-Temporal
597 Geochemistry of Mercury in Waters of the Tapajos and Amazon Rivers, Brazil. *Limnol.*
598 *Oceanogr.* 46(5), 1141-1157.

599 Roulet, M., Lucotte, M., Canuel, R., Rheault, I., Tran, S., De Freitas Gog, Y.G., Farella, N.,
600 Souza do Vale, R., Sousa Passos, C.J., De Jesus de Silva, E., Mergler, D. and Amorim,
601 M. (1998a) Distribution and partition of total mercury in waters of the Tapajos River
602 basin, Brazilian Amazon. *Sci. Total Environ.* 213, 203-211.

603 Roulet, M., Lucotte, M., Dolbec, J., Gogh, Y.F. and Pelaja, J.R.P. (1999a) 5th International
604 Conference Mercury as a Global Pollutant, Rio de Janeiro, Brazil.

605 Roulet, M., Lucotte, M., Farella, N., Serique, G., Coelho, H., Sousa Passos, C.J., De Jesus Da
606 Silva, E., Scavone De Andrade, P., Mergler, D., Guimaraes, J.R.D. and Amorim, M.
607 (1999b) Effects of recent human colonization on the presence of mercury in Amazonian
608 ecosystems. *Water Air Soil Poll.* 112, 297-313.

609 Roulet, M., Lucotte, M., Saint-Aubin, A., Tran, S., Rheault, I., Farella, N., Da Silva, E.D.,
610 Dezencourt, J., Passos, C.J.S., Soares, G.S., Guimaraes, J.R.D., Mergler, D. and
611 Amorim, M. (1998b) The geochemistry of mercury in central Amazonian soils
612 developed on the Alter-do-Chao formation of the lower Tapajos River Valley, Para
613 state, Brazil. *Sci. Total Environ.* 223(1), 1-24.

614 Soulsby, C., Tetzlaff, D., van den Bedem, N., Malcolm, I.A., Bacon, P.J. and Youngson, A.F.
615 (2007) Inferring groundwater influences on surface water in montane catchments from
616 hydrochemical surveys of springs and streamwaters. *J. hydrology* 333, 199-213.

617 Tseng, C.M., de Diego, A., Pinaly, H., Amouroux, D. and Donard, O.F.X. (1998)
618 Cryofocusing coupled to atomic absorption spectrometry for rapid and simple mercury
619 speciation in environmental matrices. *J. Anal Atom Spectro.* 13, 755-764.

620 Ullrich, S.M., Tanton, T.W. and Abdrashitova, S.A. (2001) Mercury in the aquatic
621 environment: A review of factors affecting methylation. *Crit. rev. Environ. Sci.*
622 *Technol.* 31(3), 241-293.

623 Wasserman, J.C., Hacon, S. and Wasserman, M.A. (2003) Biogeochemistry of Mercury in the
624 Amazonian Environment. *Ambio*, 336-342.

625 Webster, R. (2001) Statistics to support soil research and their presentation. *Eur. J. Soil Sci.*
626 *52(2)*, 331-340.

627
628
629

630 **List of tables:**

631

632 Table 1. Soil total mercury (HgT) median and mean concentrations, and standard error
633 of the mean (SEM) for different soil types; presented as median / mean (SEM).

634

635 Table 2. Stream water total dissolved mercury (HgT)_D, particulate mercury (HgT)_P,
636 dissolved monomethylmercury (MMHg)_D, and particulate monomethylmercury (MMHg)_P
637 median and mean concentrations, and SEM; presented as median / mean (SEM).

638

639 Table 3. Rain, throughfalls, stagnant (overlying) waters and pore hydromorphic soil
640 waters. Total dissolved mercury (HgT)_D and dissolved monomethylmercury (MMHg)_D
641 median and mean concentrations, and SEM; presented as median / mean (SEM). Subscript 1
642 relates to single location of the gold mined flat between 1 and 10 cm for stagnant waters and 0
643 to 15 cm for pore waters, and subscript 2 relates to various locations in the gold mined flat.

644

645 Table 4. Stream waters at the outlet of the pristine oxisol sub-watershed and the entire
646 watershed. Total dissolved mercury (HgT)_D, particulate mercury (HgT)_P, dissolved
647 monomethylmercury (MMHg)_D, and particulate monomethylmercury (MMHg)_P median and
648 mean specific fluxes, and SEM; presented as median / mean (SEM).

649

650

Soil type	Soil depth (cm)	HgT ($\mu\text{g g}^{-1}$)
Oxisol (pristine slopes)	0-50	0.35 / 0.37 (0.04)
	> 50	0.42 / 0.38 (0.03)
Ultisol (pristine slopes)	0-50	0.20 / 0.25 (0.07)
	> 50	0.07 / 0.10 (0.04)
Hydromorphic soil (contaminated flat)	0-50	0.82 / 1.31 (0.35)
	> 50	0.75 / 1.01 (0.26)

651

652 Table 1. Soil total mercury (HgT) median and mean concentrations, and standard error of the
653 mean (SEM) for different soil types; presented as median / mean (SEM).

654

655

Sampling location:	(HgT) _D (ng L ⁻¹)	(HgT) _P (μg g ⁻¹)	(MMHg) _D (ng L ⁻¹)	(MMHg) _P (ng g ⁻¹)
PS	0.94 / 0.98 (0.13)	0.25 / 0.53 (0.13)	0.006 / 0.016 (0.004)	1.84 / 1.86 (0.37)
MS	1.34 / 2.77 (0.75)	0.61 / 0.82 (0.17)	0.009 / 0.048 (0.033)	0.75 / 0.75 (0.67)
CO	1.57 / 4.78 (1.46)	0.88 / 1.99 (0.94)	0.056 / 0.062 (0.005)	6.80 / 9.59 (1.28)
BR	1.67 / 4.94 (3.43)	1.51 / 1.42 (0.33)	0.024 / 0.025 (0.004)	1.69 / 2.67 (1.33)

656

657 Table 2. Stream water total dissolved mercury (HgT)_D, particulate mercury (HgT)_P, dissolved
658 monomethylmercury (MMHg)_D, and particulate monomethylmercury (MMHg)_P median and
659 mean concentrations, and SEM; presented as median / mean (SEM).

660

661

Sampling location:	(HgT) _D (ng L ⁻¹)	(HgT) _P (μg g ⁻¹)	(MMHg) _D (ng L ⁻¹)	(MMHg) _P (ng g ⁻¹)
PS	0.94 / 0.98 (0.13)	0.25 / 0.53 (0.13)	0.006 / 0.016 (0.004)	1.84 / 1.86 (0.37)
MS	1.34 / 2.77 (0.75)	0.61 / 0.82 (0.17)	0.009 / 0.048 (0.033)	0.75 / 0.75 (0.67)
CO	1.57 / 4.78 (1.46)	0.88 / 1.99 (0.94)	0.056 / 0.062 (0.005)	6.80 / 9.59 (1.28)
BR	1.67 / 4.94 (3.43)	1.51 / 1.42 (0.33)	0.024 / 0.025 (0.004)	1.69 / 2.67 (1.33)

662

663

664 Table 2. Stream water total dissolved mercury (HgT)_D, particulate mercury (HgT)_P, dissolved
665 monomethylmercury (MMHg)_D, and particulate monomethylmercury (MMHg)_P median and
666 mean concentrations, and SEM; presented as median / mean (SEM).

667

Sampling location	(HgT) _D (ng L ⁻¹)	(MMHg) _D (ng L ⁻¹)
Rain (PS)	4.83 / 4.63 (0.74)	0.010 / 0.011 (0.003)
Throughfall (PS)	3.98 / 3.93 (0.68)	0.017 / 0.026 (0.008)
Soil overlying water (Pristine subwatershed)	1.70 / 3.11 (1.25)	0.005 / 0.007 (0.002)
Soil overlying water ¹ (Contaminated flat)	-	0.615 / 0.670 (0.080)
Soil overlying water ² (Contaminated flat)	2.01 / 2.01 (0.40)	0.082 / 0.243 (0.098)
Soil pore water ¹ (Contaminated flat)	-	0.136 / 0.113 (0.034)
Soil pore water ² (Contaminated flat)	2.34 / 5.49 (1.65)	0.161 / 0.231 (0.047)

669

670

671 Table 3. Rain, throughfalls, stagnant (overlying) waters and pore hydromorphic soil waters.

672 Total dissolved mercury (HgT)_D and dissolved monomethylmercury (MMHg)_D median and

673 mean concentrations, and SEM; presented as median / mean (SEM). Subscript 1 relates to

674 single location of the gold mined flat between 1 and 10 cm for stagnant waters and 0 to 15 cm

675 for pore waters, and subscript 2 relates to various locations in the gold mined flat.

676

677

Specific fluxes	PS	CO
	(surface 0.12 km ²)	(surface 1.27 km ²)
(HgT) _D (ng s ⁻¹ km ⁻²)	113 / 147 (32)	117 / 628 (276)
(HgT) _P (ng s ⁻¹ km ⁻²)	517 / 1458 (521)	1104 / 2951 (1158)
(MMHg) _D (ng s ⁻¹ km ⁻²)	0.67 / 0.97 (0.30)	4.20 / 4.17 (0.51)
(MMHg) _P (ng s ⁻¹ km ⁻²)	3.5 / 4.2 (0.96)	14.0 / 21.6 (3.80)

678

679 Table 4. Stream waters at the outlet of the pristine oxisol sub-watershed and the entire
680 watershed. Total dissolved mercury (HgT)_D, particulate mercury (HgT)_P, dissolved
681 monomethylmercury (MMHg)_D, and particulate monomethylmercury (MMHg)_P median and
682 mean specific fluxes, and SEM; presented as median / mean (SEM).

683

684 **Figure captions**

685

686 Figure 1. The watershed study site with water sampling (PS – pristine spring, MS –
687 middlestream and CO - contaminated flat outlet, in the Combat Creek and BR-
688 Boulanger River), soil sampling locations and soil types (O: oxisol, U: ultisol
689 and H: hydromorphic soil).

690

691 Figure 2. Dissolved $[(\text{HgT})_{\text{D}}]$ and $[(\text{MMHg})_{\text{D}}]$ versus $[\text{Cl}^-]$, for rain, throughfall and
692 stream waters at each sampling location; PS, MS and CO respectively, sampled
693 during and out of rain events at the 3 sampling points (PS, MS and CO) and at
694 the beginning and the middle of the rainy season, respectively.

695

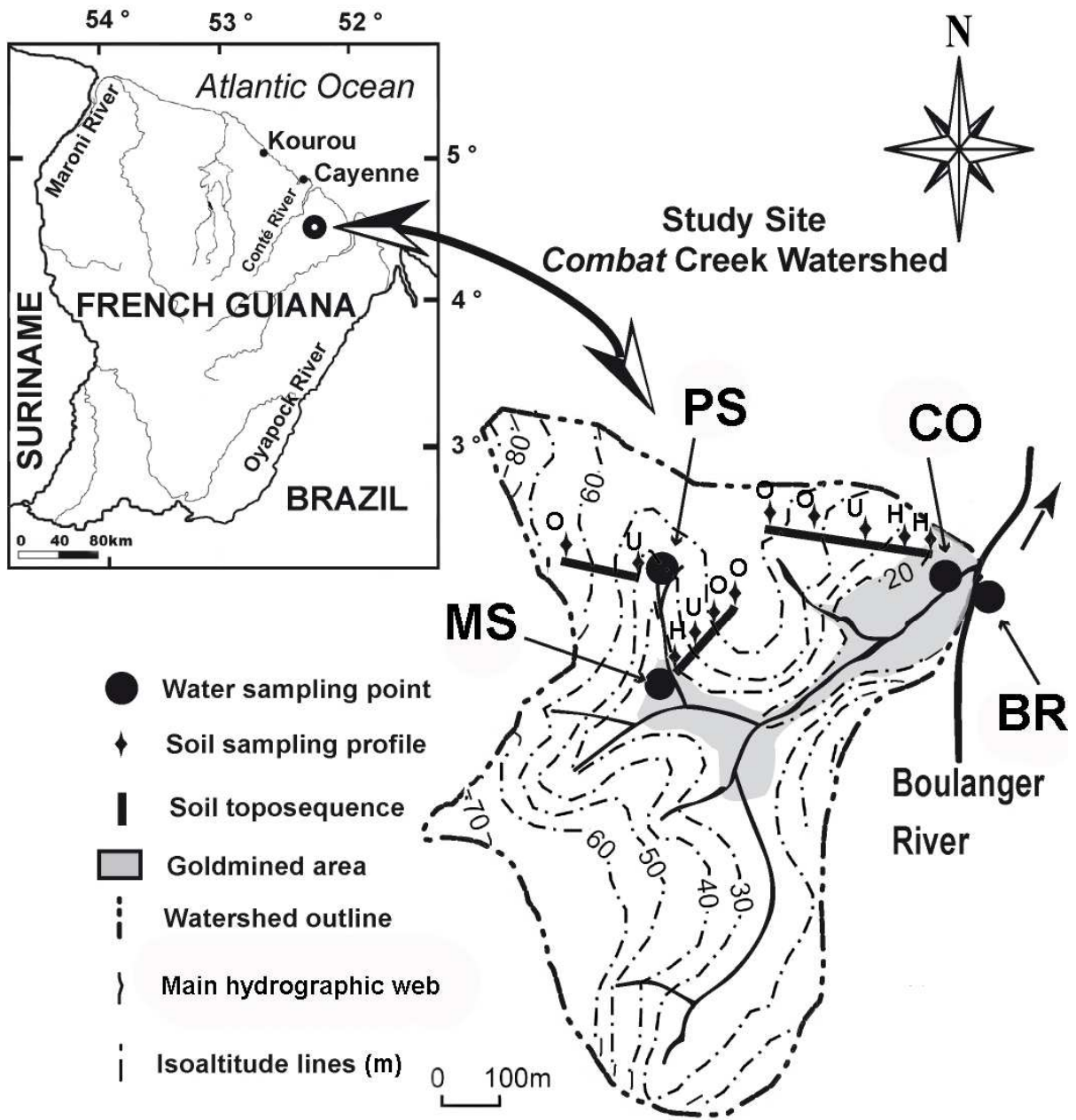
696 Figure 3. $[(\text{MMHg})_{\text{D}}]$ and $[(\text{HgT})_{\text{D}}]$ versus Eh and $[\text{Fe}^{\text{II}}]$ in soil waters. Soil pore waters
697 and overlying waters were sampled near the PS and in the former gold mined
698 area between MS and CO, in the beginning and middle of the rainy season.
699 Regression lines are plotted if significant ($p < 0.05$).

700

701 Figure 4. $[(\text{MMHg})_{\text{D}}]$ (ng L^{-1}), $[\text{Fe}^{\text{II}}]$ (mg L^{-1}), and Eh (mV) vertical profiles and sulfide-
702 accumulating zone (SAZ - gray color area) of the overlying (10 cm thick water
703 puddle) and pore water of a flooded hydromorphic soil in the former gold
704 mined area between MS and CO, at the beginning of the rainy season. Soil-
705 water interface (0cm) is plotted as a horizontal line.

706

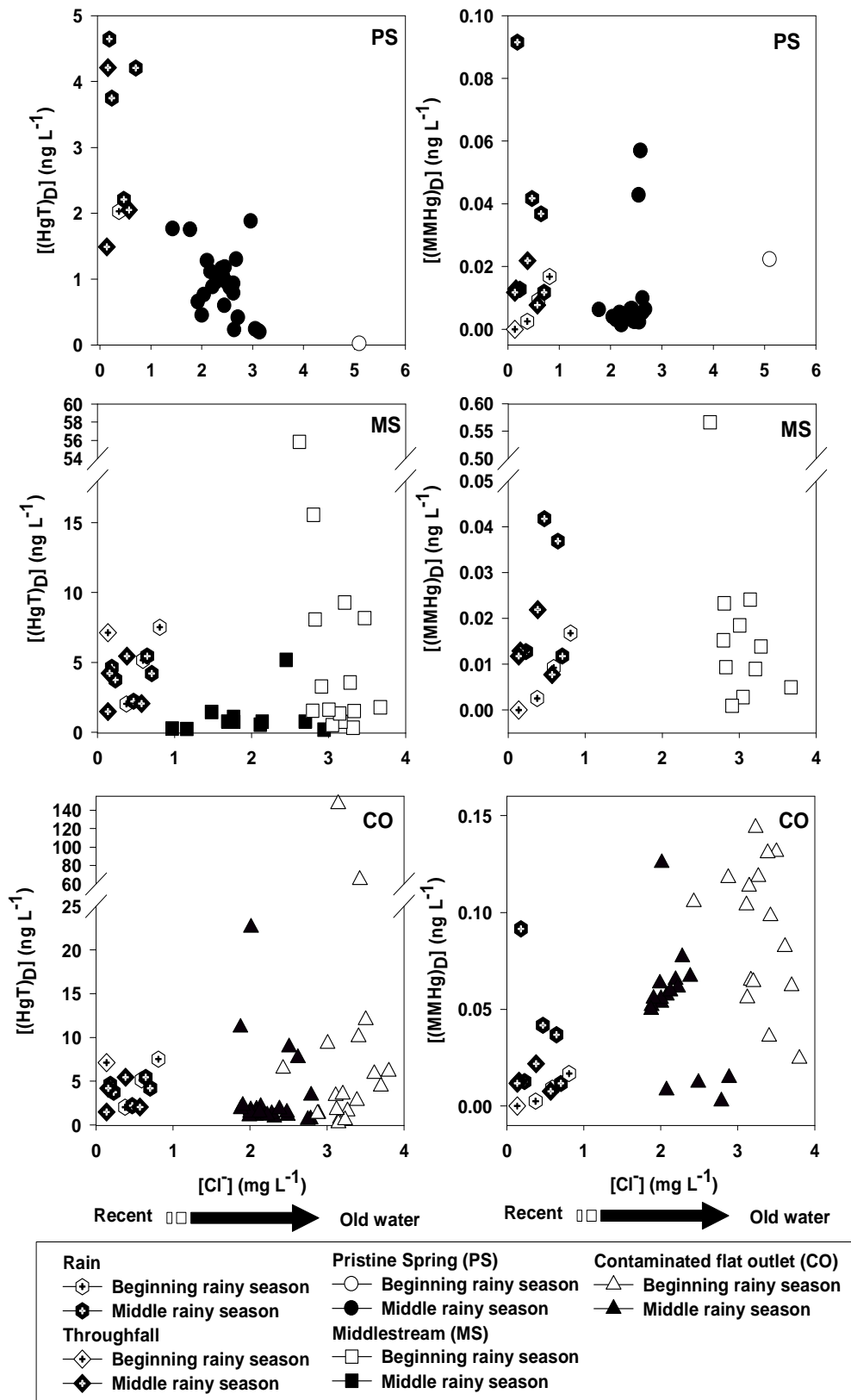
707 Figure 1.



708

709

710 Figure 2.

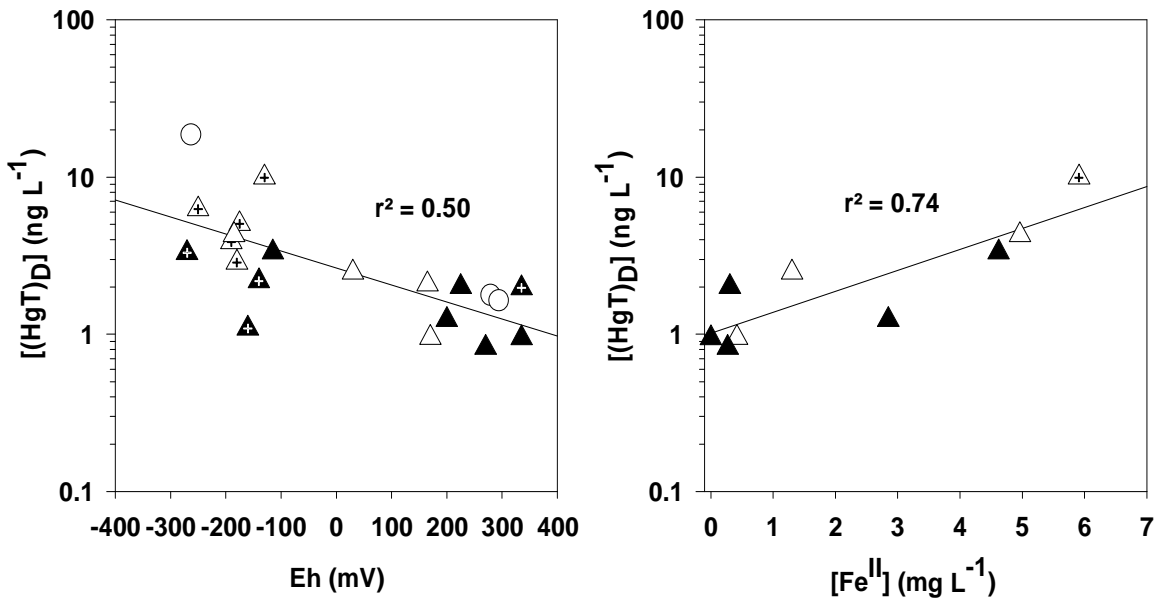
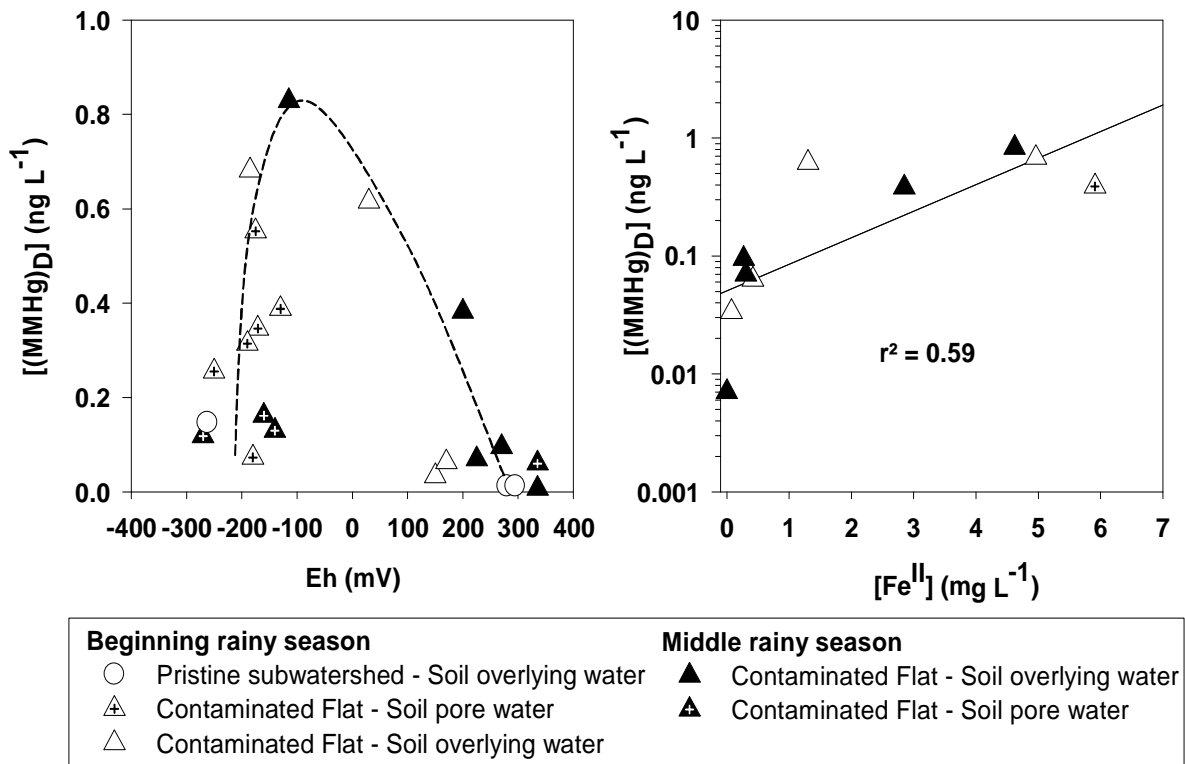


711

712

713 Figure 3.

714



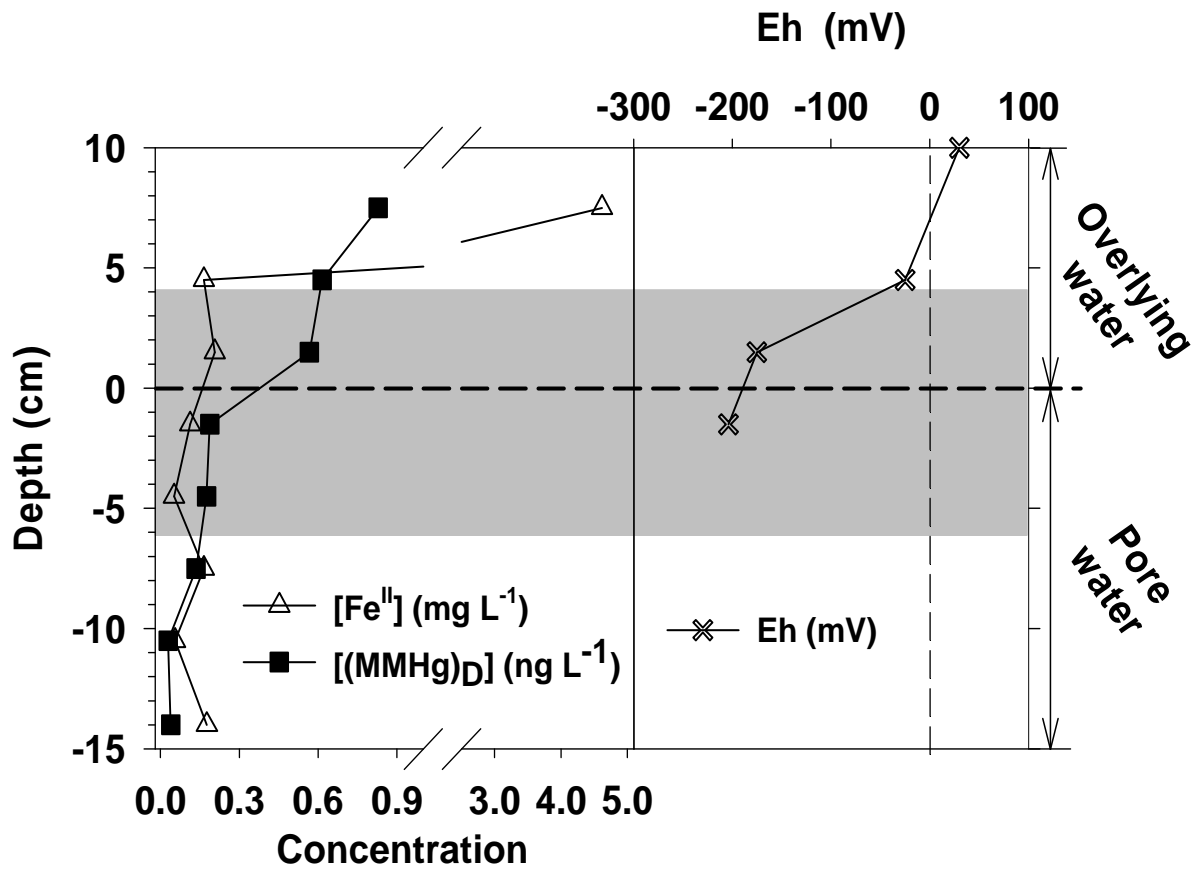
715

716

717 Figure 4.

718

719



720